PCCP

Evaluation of Hydrogen Storage in Sandstone Reservoirs using 1H Nuclear Magnetic Resonance Spectroscopy

Journal:	*Physical Chemistry Chemical Physics*
Manuscript ID	CP-COM-11-2024-004366.R1
Article Type:	Communication
Date Submitted by the Author:	10-Dec-2024
Complete List of Authors:	Dang, Son; University of Oklahoma Mamoudou, Sidi; University of Oklahoma Rai, Chandra; University of Oklahoma Ho, Tuan; Sandia National Laboratories, Geochemistry

SCHOLARONE™ Manuscripts

PCCP

Evaluation of Hydrogen Storage in Sandstone Reservoirs using [1]H Nuclear Magnetic Resonance Spectroscopy

Son T. Dang[a]†, Sidi Mamoudou [a], Chandra S. Rai[a], and Tuan A. Ho[b]†

Evaluation of hydrogen storage capacity of porous rocks is crucial for underground hydrogen storage. Using [1]H Nuclear Magnetic Resonance (NMR) spectroscopy we successfully characterized the hydrogen responses and identified storage mechanisms in Berea sandstone under varying water saturation. The results indicate that the injected hydrogen behaves as a free gas phase and is capable of occupying the empty pore volume regardless of saturation state. No hysteresis was observed during injection and production cycles.

Hydrogen geological storage (HGS) has the potential to play a crucial role in the future transition to a hydrogen-based economy and in meeting net-zero emissions targets. While HGS in salt caverns is proven technology, HGS in depleted oil/gas reservoirs and deep saline aquifers remains uncertain. Nonetheless, depleted oil/gas reservoirs and aquifers are particularly desirable because they offer geographic flexibility and existing infrastructure. To reduce the uncertainty of HGS in depleted oil/gas reservoirs and aquifers, recent research has focused on identifying potential alterations in reservoirs following H_2 injection, such as changes in mineral wettability,[1-3] gas solubility,[4] mineral dissolution,[5, 6] fluid transport properties of surrounding rocks,[7] redox reactions, e.g., reduction of Fe(III) in clays to Fe(II)[8] and pyrite into pyrrhotite,[9] abiotic geochemical reactions in sandstone reservoirs,[10, 11] thermo-physical properties of hydrogen interactions with other gaseous species,[12] and microbial activities.[13-17] These alterations may impact the technical and economic feasibility of HGS. Our recent work has focused on using ^{1}H NMR spectroscopy, adsorption experiments, and molecular simulations to investigate hydrogen loss mechanisms after injection into an underground reservoir. [18-20]

Few studies have focused on understanding the hydrogen storage capacity as a function of water saturation in sandstone reservoirs, highlighting the need to develop reliable tools to evaluate both storage capacity and dynamic interactions among injected hydrogen, rock, and *in-situ* reservoir fluids. These tools must be thoroughly tested under laboratory conditions before being applied in field-scale characterization.

In the oil and gas industry, ^{1}H NMR spectroscopy, which responds to hydrogen protons in formation brine, hydrocarbons, and clay hydroxyl groups, has proven valuable for understanding porous media storage mechanisms, fluid identification, and rock-fluid interactions.[21-24] This technology has been widely accepted and has evolved from laboratory studies to downhole measurements.[25, 26] Previous work has demonstrated that low-field NMR can be used to determine free and adsorbed methane phases in coal[27] and shales.[22, 28, 29] More recently, we utilized NMR to study H_2 in shales and identified distinctive NMR relaxation signatures of H_2 in porous materials. [18] The fact that ^{1}H NMR responds to hydrogen gas makes it one of the few powerful tools for understanding HGS at both laboratory and field scales.

In this study, we used ^{1}H NMR spectroscopy to demonstrate the unique chemical response of hydrogen in Berea sandstone under varying water saturations. We present the ^{1}H NMR responses of bulk hydrogen gas, and water and hydrogen in partially saturated Berea sandstone. This work highlights the potential of using ^{1}H NMR spectroscopy for field-scale characterization of hydrogen storage in sandstone reservoirs.

In Fig. 1 we present the T_2 relaxation distribution of bulk H_2 at 300 K as a function of gas pressure. The experimental apparatus and procedure are detailed in our previous work. [18] Briefly, the NMR T_2 relaxation distribution was acquired at the frequency of 2 MHz using an NMR spectrometer with the Carr - Purcell-Meiboom-Gill (CPMG) sequence.[30, 31] The magnet temperature was set at 300 K throughout the experiments. Both bulk H_2 and sample injection tests were performed inside a

[a.] *Mewbourne School of Petroleum and Geological Engineering, The University of Oklahoma, Norman, OK 73019, USA*
[b.] *Geochemistry Department, Sandia National Laboratories, Albuquerque, NM 87185, USA.*
† *Corresponding authors: dangthaison@ou.edu and taho@sandia.gov*

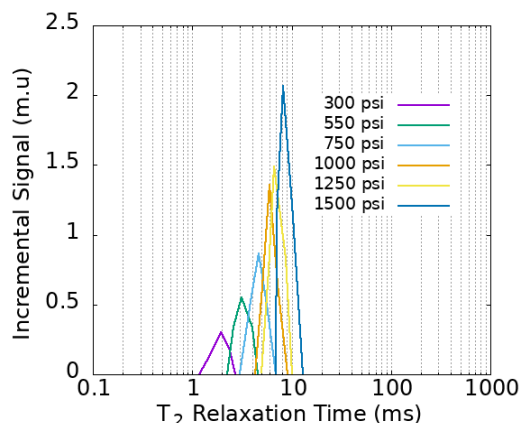Daedalus® core holder made of NMR transparent ZrO_2. The cell

Figure 1 NMR T_2 relaxation distribution of bulk H_2 at different pressures up to 1500 psi at 300 K.

can be operated up to 10,000 psi internal pressure. During the NMR sequence, the released nuclear spin energy during the relaxation phase is captured, and the total signal is proportional to the molar density of hydrogen atoms within the investigated volume. Note that the result shown in Fig. 1 is the conversion of NMR signal of compressed hydrogen gas in machine units. The NMR T_2 relaxation of bulk H_2 with an empty ZrO_2 cell, as the pressure varies up to 1500 psi, shows that bulk hydrogen relaxes within the range of 1-50 ms. An increase in amplitude with pressure and a shift in the mean T_2 to higher relaxation times are observed. The same behavior has been reported for hydrocarbon gases such as methane;[27, 32, 33] however at a longer T_2 relaxation time (200-1000 ms).
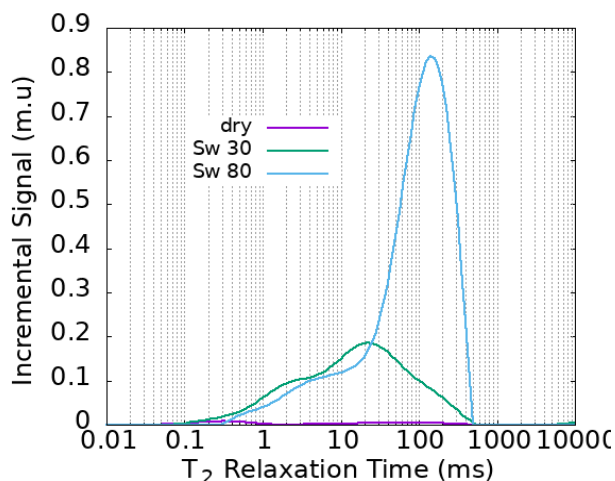

Figure 2. NMR T_2 relaxation for the Berea sandstone at dried, and partially saturated conditions, and the illustration for water distributed within different pore sizes.

To investigate the interactions between injected hydrogen and *in situ* fluids within storage reservoirs, we saturated Berea sandstone to achieve water saturations (Sw) of 30% and 80% [i.e., gas saturation (Sg) of 70% and 20%, respectively] before performing hydrogen injection tests with real time NMR monitoring. A Berea core plug approximately 2.5 inches long and 1 inch in diameter was used in this study. Before water

saturation and NMR measurements, the specimen was cleaned by Soxhlet extraction with toluene-methanol (80:20) mixture for 3 weeks and then dried in an oven at 100 °C for one week. Gas-filled porosity of 21% was measured by Helium expansion.
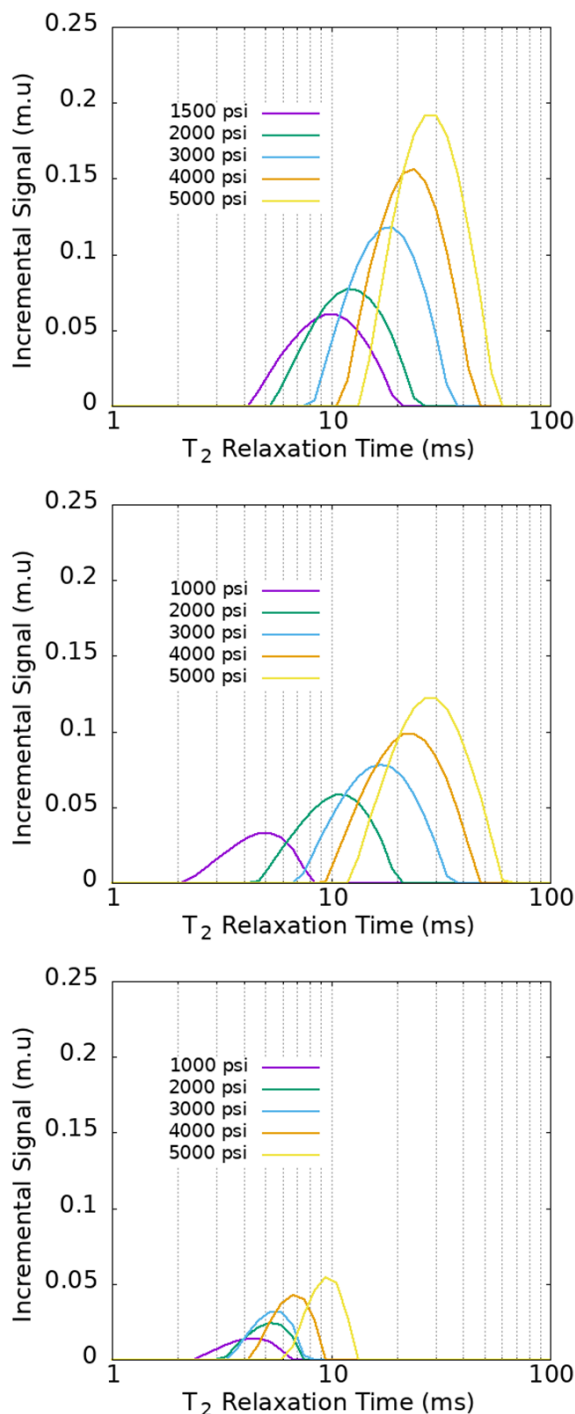

Figure 3. NMR T_2 distribution of H_2 in Berea sandstone at different saturations, Sw = 0 (top), 30% (middle), and 80% (bottom).

Mineralogy was determined with transmission Fourier–transform infrared spectroscopy.[34] The sample mainly contains quartz (86 w%), kaolinite clay (10 w%), and some other trace minerals.

Fig. 2 shows the NMR T_2 distribution of water within Berea pore volume at different Sw. Note that the signal for the dry sample is negligible, indicating the insignificant contribution of clay protons (or hydroxyl groups). The NMR responses of water in Berea are different from the NMR T_2 response of bulk water which is from 2000 to 3000 ms. At a low Sw, water is capillary-bound, resulting in short T_2 values. As Sw increases, T_2 relaxation time shifts to longer values with higher amplitude. Therefore, the T_2 relaxation time is positively correlated with the pore size, e.g., at a lower Sw, most of water occupies smaller pores. The raw decay signals of these distributions will serve as the baseline for further investigation of T_2 distribution of H_2 injected into the rock sample at a specific Sw.

We then inject H_2 into dry and partially saturated Berea
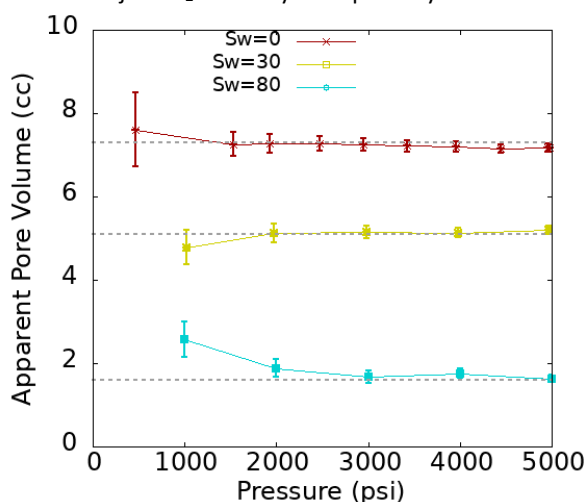

Figure 4. Apparent pore volume occupied by H_2 calculated using hydrogen index and NMR data at different pressure. Dashed lines are the pore volume not occupied by water (i.e., Sg) at different Sw. The volume filled by H_2 matches well with the volume not occupied by water.

sandstone and monitor the total NMR response as a function of gas pressure. In Fig. 3 we report the NMR T_2 distribution of H_2 after subtracting the background signal, e.g., responses in Fig. 2. The results indicate that, regardless of saturation conditions, the signal from H_2 intake appears to be in a similar T_2 relaxation time range as bulk H_2 (Fig. 1), e.g., T_2 distribution is between 1 and 50 ms and longer T_2 relaxation times at higher pressures. The total signal also increases because more gas molecules are trapped in the same remaining pore volumes. However, the influence of water saturation is inevitable. At the same gas pressure, for example at 5000 psi, the peak of the T_2 relaxation for H_2 shifts to a shorter T_2 value and the magnitude decreases when water saturation increases. At a higher Sw, most of the pore volume is occupied by water as the wetting phase, leaving less space for H_2 storage, which is reflected in the T_2 relaxation time.

We now calculate the pore volume occupied by injected H_2 using the results in Fig. 3 and hydrogen index for H_2 gas at a specific pressure. Fig. 4 shows the apparent pore volume occupied by injected H_2 within rock matrix at dry and different Sw. The difference between total pore volume and H_2-occupied

closely matches the volume of water saturation, suggesting that H_2 can easily flow through partially saturated rock and fill in empty pore space, regardless of Sw. In other words, hydrogen storage capacity is linearly proportional to the Sg. In general, at high Sw, water blockage at pore throats limits the gas (e.g., CO_2, N_2) intrusion into the pores leading to lower gas storage capacity, compared to available Sg. However, our results for Berea sandstone indicate that this is not the case for hydrogen.

In Fig. 5 we report the NMR responses of hydrogen intake during injection (loading) and production (unloading) for both dry and Sw=80%. The results show insignificant hysteresis for both cases, indicating that hydrogen can be fully recovered after injection. This observation may be due to the uniformity of Berea's pore size distribution and absence of the adsorption effects in nanopores. Note that hysteresis was observed for shale sample in our previous work.[18] We expect that samples with smaller pores and higher heterogeneity in pore size distribution, compared to Berea sandstone, might exhibit hysteresis due to viscous fingering.

All observations in this study can potentially be used to interpret hydrogen storage capacity and behavior within reservoir rocks using downhole NMR wireline measurements.
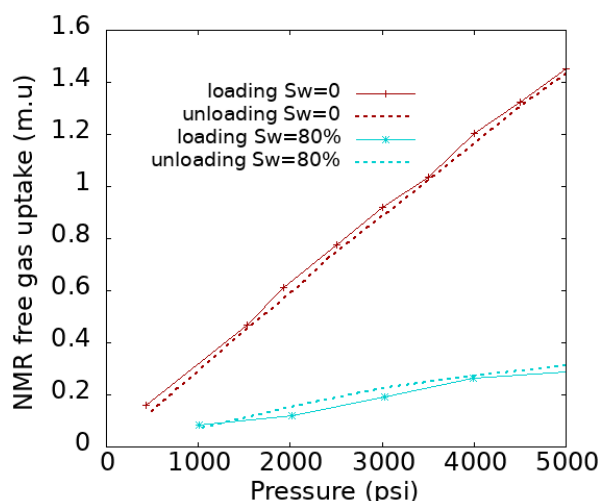

Figure 5. H_2 intake between loading and unloading of H_2 into dried (Sw=0) and partially saturated (Sw = 80%) Berea sandstone. Insignificant hysteresis is observed regardless of water saturation.

The results also indicate a significant potential for storage in depleted gas reservoirs, where water saturation can be low. In such cases, storage capacity can be effectively calculated from Sw, and stored hydrogen can be efficiently recovered.

Conflicts of interest

There are no conflicts to declare.

Notes and references

1. L. Zeng, M. Hosseini, A. Keshavarz, S. Iglauer, Y. Lu and Q. Xie, *International Journal of Hydrogen Energy*, 2022, **47**, 25357-25366.
2. S. Higgs, Y. Da Wang, C. Sun, J. Ennis-King, S. J. Jackson, R. T. Armstrong and P. Mostaghimi, *International Journal of Hydrogen Energy*, 2022, **47**, 13062-13075.
3. B. Pan, K. Liu, B. Ren, M. Zhang, Y. Ju, J. Gu, X. Zhang, C. R. Clarkson, K. Edlmann, W. Zhu and S. Iglauer, *Fuel*, 2023, **333**, 126516.
4. S. Chabab, P. Théveneau, C. Coquelet, J. Corvisier and P. Paricaud, *International Journal of Hydrogen Energy*, 2020, **45**, 32206-32220.
5. J. P. Bensing, D. Misch, L. Skerbisch and R. F. Sachsenhofer, *International Journal of Hydrogen Energy*, 2022, **47**, 30621-30626.
6. A. Al-Yaseri, H. Al-Mukainah, N. Yekeen and A. S. Al-Qasim, *International Journal of Hydrogen Energy*, 2023, **48**, 3583-3592.
7. M. Ghasemi, S. Omrani, S. Mahmoodpour and T. Zhou, *International Journal of Hydrogen Energy*, 2022, **47**, 24871-24885.
8. M. Didier, L. Leone, J.-M. Greneche, E. Giffaut and L. Charlet, *Environmental Science & Technology*, 2012, **46**, 3574-3579.
9. L. Truche, M.-C. Jodin-Caumon, C. Lerouge, G. Berger, R. Mosser-Ruck, E. Giffaut and N. Michau, *Chemical Geology*, 2013, **351**, 217-228.
10. A. Hassanpouryouzband, K. Adie, T. Cowen, E. M. Thaysen, N. Heinemann, I. B. Butler, M. Wilkinson and K. Edlmann, *ACS Energy Letters*, 2022, **7**, 2203-2210.
11. A. E. Yekta, M. Pichavant and P. Audigane, *Applied Geochemistry*, 2018, **95**, 182-194.
12. A. Hassanpouryouzband, E. Joonaki, K. Edlmann, N. Heinemann and J. Yang, *Scientific Data*, 2020, **7**, 222.
13. N. Heinemann, J. Alcalde, J. M. Miocic, S. J. T. Hangx, J. Kallmeyer, C. Ostertag-Henning, A. Hassanpouryouzband, E. M. Thaysen, G. J. Strobel, C. Schmidt-Hattenberger, K. Edlmann, M. Wilkinson, M. Bentham, R. Stuart Haszeldine, R. Carbonell and A. Rudloff, *Energy & Environmental Science*, 2021, **14**, 853-864.
14. P. Šmigáň, M. Greksák, J. Kozánková, F. Buzek, V. Onderka and I. Wolf, *FEMS Microbiology Ecology*, 1990, **73**, 221-224.
15. F. Buzek, V. Onderka, P. Vančura and I. Wolf, *Fuel*, 1994, **73**, 747-752.
16. M. Berta, F. Dethlefsen, M. Ebert, D. Schäfer and A. Dahmke, *Environmental Science & Technology*, 2018, **52**, 4937-4949.
17. P. G. Haddad, M. Ranchou-Peyruse, M. Guignard, J. Mura, F. Casteran, L. Ronjon-Magand, P. Senechal, M. P. Isaure, P. Moonen, G. Hoareau, D. Dequidt, P. Chiquet, G. Caumette, P. Cezac and A. Ranchou-Peyruse, *Energy & Environmental Science*, 2022, **15**, 3400-3415.
18. T. A. Ho, S. T. Dang, N. Dasgupta, A. Choudhary and Y. Wang, *International Journal of Hydrogen Energy*, 2023, **51**, 158-166.
19. T. A. Ho, C. F. Jove-Colon and Y. Wang, *Sustainable Energy & Fuels*, 2023, **7**, 3232-3238.
20. A. Choudhary and T. A. Ho, *Physical Chemistry Chemical Physics*, 2024, **26**, 10506-10514.
21. E. Odusina, C. Sondergeld and C. Rai, *Canadian Unconventional Resources Conference*, 2011, **SPE-147371-MS**.
22. A. Tinni, E. Odusina, I. Sulucarnain, C. Sondergeld and C. S. Rai, *SPE Reservoir Evaluation & Engineering*, 2015, **18**, 400-406.
23. M. Fleury and M. Romero-Sarmiento, *Journal of Petroleum Science and Engineering*, 2016, **137**, 55-62.
24. S. T. Dang, C. H. Sondergeld and C. S. Rai, *SPE Reservoir Evaluation & Engineering*, 2018, **22**, 302-309.
25. W. E. Kenyon, P. I. Day, C. Straley and J. F. Willemsen, *SPE Formation Evaluation*, 1988, **3**, 622-636.
26. G. R. Coates, R. C. A. Peveraro, A. Hardwick and D. Roberts, *SPE Annual Technical Conference and Exhibition*, 1991, **SPE-22723-MS**.
27. Y. Yao, D. Liu and S. Xie, *International Journal of Coal Geology*, 2014, **131**, 32-40.
28. Y. Yao, J. Liu, D. Liu, J. Chen and Z. Pan, *International Journal of Coal Geology*, 2019, **201**, 76-85.
29. R. Kausik, C. C. Minh, L. Zielinski, B. Vissapragada, R. Akkurt, Y. Song, C. Liu, S. Jones and E. Blair, *SPE Annual Technical Conference and Exhibition*, 2011, **SPE-147198-MS**.
30. H. Y. Carr and E. M. Purcell, *Physical Review*, 1954, **94**, 630-638.
31. S. Meiboom and D. Gill, *Review of Scientific Instruments*, 1958, **29**, 688-691.
32. C. J. Gerritsma and N. J. Trappeniers, *Physica*, 1971, **51**, 365-380.
33. R. Akkurt, A. J. Guillory, P. N. Tutunjian and H. J. Vinegar, *The Log Analyst*, 1996, **37**.
34. C. H. Sondergeld and C. S. Rai, in *Experimental Techniques in Mineral and Rock Physics: The Schreiber Volume*, eds. R. C. Liebermann and C. H. Sondergeld, Birkhäuser Basel, Basel, 1994, pp. 249-268.

All data used in this article have been provided in Figures 1-5.